86ER13510), by the Pittsburgh Energy Technology Center through the Consortium for Fossil Fuel Liquefaction Science (Contract No. DE-FC22-89PC89852), and by the National Science Foundation through the Advanced Combustion Engineering Research Center (Cooperative Agreement No. CDR8522618). Computer time on the IBM 3090-600S of the Utah Supercomputing Institute, funded by the State of Utah and the IBM Corporation, is also gratefully acknowledged.

Catalysis by Heteropoly Compounds. 20.† An NMR Study of Ethanol Dehydration in the Pseudoliquid Phase of 12-Tungstophosphoric Acid

Kwan Young Lee,‡ Takeo Arai,‡,‖ Shin-ichi Nakata,§ Sachio Asaoka,§ Toshio Okuhara,‡ and Makoto Misono*,‡

Contribution from the Department of Synthetic Chemistry, Faculty of Engineering, The University of Tokyo, Bunkyo-ku, Tokyo 113, Japan, and R&D Center, Chiyoda Corporation, Kanagawa-ku, Yokohama 221, Japan. *Received August 14, 1991*

Abstract: Dehydration of ethanol in the pseudoliquid phase of 12-tungstophosphoric acid, $H_3PW_{12}O_{40}$, was studied by means of solid-state NMR combined with IR, thermal desorption, and transient-response methods. It was confirmed by the transient-response method using isotopically labeled ethanol that a large amount of ethanol was absorbed in the lattice of the catalyst bulk (pseudoliquid phase) under the reaction conditions, and the reaction proceeded in the bulk phase. Probable reaction intermediates of the ethanol dehydration such as protonated ethanol dimer ($(C_2H_5OH)_2H^+$) and monomer ($C_2H_5OH_2^+$) were directly identified in this phase by solid-state NMR spectroscopy. The assignments were supported by IR spectroscopy and stoichiometry of ethanol absorption. By comparison of the NMR data with the results of thermal desorption of ethanol, the dimer and monomer species are very likely the intermediates for diethyl ether and ethylene formation, respectively. The unusual pressure dependence observed for the dehydration of ethanol was reasonably explained by the changes in the concentration of these intermediates in the pseudoliquid phase.

Introduction

Heteropoly acids are good cluster models of mixed oxide catalysts, and their catalyses can be described at the molecular level.[1-5] At the same time, they are good starting materials for catalyst design based on their acid and redox properties.[5] In fact, heteropoly compounds are used as catalysts for several industrial processes[6] such as oxidation of methacrolein, hydrations of propene, *n*-butene, and 2-methylpropene, and polymerization of tetrahydrofuran.

A very remarkable property of the heteropoly acids when they are used as solid catalysts is the formation of a "pseudoliquid phase" that we reported earlier.[7] Higher activities of $H_3PW_{12}O_{40}$ at low temperatures for dehydration of alcohols,[8-10] etherification,[11] esterification,[12] alkylation,[13] and decomposition of ester[14] than of SiO_2-Al_2O_3 and other solid acids are closely related to this property. Polar molecules like H_2O, alcohols, and ethers readily move into or out of the three-dimensional bulk phase, sometimes expanding or shrinking the distance between the anions.[7,15,16] This behavior is due to the flexible nature of the secondary structure (or the three-dimensional arrangement of polyanions, counter cations, etc.) of the heteropoly acid in the solid state.[5] This is not the adsorption in the micropores of the heteropoly acids (there are no micropores in the crystal structure[17]). A large number of alcohols were readily absorbed during the dehydration,[18,19] as revealed by the transient-response analysis using isotopically labeled alcohols. This pseudoliquid phase behavior brought about high catalytic activities for a variety of reactions as cited above.[8-14,20,21] Besides the activities, unique selectivities for dehydration of ethanol[22] and conversion of dimethyl ether to hydrocarbons[23] have been reported.

† Part 19: Mizuno, N., et al. *Nippon Kagaku Kaishi* **1991**, 1066-1072. This work was partly supported by a Grant-in-Aid for Scientific Research from the Ministry of Education, Science and Culture of Japan.

‡ Department of Synthetic Chemistry, The University of Tokyo.
§ Chiyoda Corporation.
‖ Present address: Konica Co. Inc., Japan.

(1) (a) Pope, M. T.; Muller, A. *Angew. Chem., Int. Ed. Engl.* **1991**, *30*, 34-48. (b) Pope, M. T. *Heteropoly and Isopoly Oxometallates*; Springer: Berlin, 1983.
(2) Tsigdinos, G. A. *Top. Curr. Chem.* **1978**, *76*, 1-64.
(3) (a) Day, V. W.; Klemperer, W. G.; Schwartz, C. *J. Am. Chem. Soc.* **1987**, *109*, 6030-6044. (b) Day, V. W.; Fredric, M. F.; Klemperer, W. G.; Liu, R.-S. *J. Am. Chem. Soc.* **1979**, *101*, 491-492.
(4) (a) Lyon, D. K.; Finke, R. G. *Inorg. Chem.* **1990**, *29*, 1787-1789. (b) Mizuno, N.; Lyon, D. K.; Finke, R. G. *J. Catal.* **1991**, *128*, 84-91.
(5) (a) Misono, M. *Catal. Rev. Rel. Subj.* **1987**, *29*, 269-321; **1988**, *30*, 339-340. (b) Misono, M. *Mater. Chem. Phys.* **1987**, *17*, 103-120.
(6) Misono, M.; Nojiri, N. *Appl. Catal.* **1990**, *64*, 1-30.
(7) (a) Misono, M., et al. CSJ/ACS Chemical Congress, Honolulu, 1979: 1st Japan-France Seminar on Catalysis, Lyon, 1979. (b) Misono, M.; Sakata, K.; Yoneda, Y.; Lee, W. Y. *Proceedings of the 7th International Congress on Catalysis, 1980*; Kodansha(Tokyo)-Elsevier(Amsterdam), 1981; pp 1047-1059.
(8) Okuhara, T.; Mizuno, N.; Lee, K. Y.; Misono, M. *Acid-Base Catalysis*; Tanabe, K., Hattori, H., Yamaguchi, T., Tanaka, T., Eds.; Kodansha: Tokyo, 1989; pp 421-438.
(9) Saito, Y.; Cook, P. N.; Niiyama, H.; Echigoya, E. *J. Catal.* **1985**, *95*, 49-56.
(10) Highfield, J. G.; Moffat, J. B. *J. Catal.* **1985**, *95*, 108-119; **1986**, *98*, 245-258.
(11) Igarashi, S.; Matsuda, T.; Ogino, Y. J. *Jpn. Petrol. Inst.* **1979**, *22*, 331-335.
(12) Izumi, Y.; Hasebe, R.; Urabe, K. *J. Catal.* **1983**, *84*, 402-409.
(13) Okuhara, T.; Kasai, A.; Hayakawa, N.; Yoneda, Y.; Misono, M. *Shokubai (Catalyst)* **1980**, *22*, 226-228.
(14) Okuhara, T.; Nishimura, T.; Ohashi, K.; Misono, M. *Chem. Lett.* **1990**, 1201-1202.
(15) Misono, M.; Mizuno, N.; Katamura, K.; Kasai, A.; Konishi, Y.; Sakata, K.; Okuhara, T.; Yoneda, Y. *Bull. Chem. Soc. Jpn.* **1982**, *55*, 400-406.
(16) Okuhara, T.; Tatematsu, S.; Lee, K. Y.; Misono, M. *Bull. Chem. Soc. Jpn.* **1989**, *62*, 717-723.
(17) Mizuno, N.; Misono, M. *Chem. Lett.* **1987**, 967-970.
(18) Okuhara, T.; Hashimoto, T.; Misono, M.; Yoneda, Y.; Niiyama, H.; Salto, Y.; Echigoya, E. *Chem. Lett.* **1983**, 573-576.

0002-7863/92/1514-2836$03.00/0

Recently, by using FTIR and solid-state NMR, we directly observed protonated ethanol molecules in the pseudoliquid phase of $H_3PW_{12}O_{40}$.[24] The elucidation of their reactivity and roles in the catalysis is the major theme of this study.

Solid-state NMR spectroscopy has great potential to become a powerful tool in the identification of reaction intermediates in heterogeneous catalysis. There have been attempts to detect alkyl cations by using solid-state ^{13}C NMR,[25-30] although the detection is still controversial.[27] Solid-state NMR has also been applied to the structural studies of heteropoly compounds[31-34] and in identifying the acid sites of silica and silica-alumina.[35,36]

In the present study, we studied the chemical state and reactivity of ethanol molecules absorbed in the pseudoliquid phase of $H_3PW_{12}O_{40}$, in relation to the mechanism of catalytic dehydration, by using high resolution solid-state NMR combined with IR, kinetics, transient-response, and thermal desorption methods.

Experimental Section

Materials. $H_3PW_{12}O_{40}\cdot nH_2O$ was purchased from Nippon Inorganic Color and Chemical Co. and was purified by extraction with diethyl ether and recrystallized from water at room temperature.[20] $H_3PW_{12}O_{40}\cdot 23H_2O$ thus prepared was stored in a sealed glass bottle at room temperature. Ethanol (Amakasu Chemical Ind.; research grade), [1,2-^{13}C]ethanol (MSD Isotopes Co., 99 atom % ^{13}C), and ethanol-d_6 (Aldrich Chemical Co., >99% deuterium) were used without further purification. $(^{13}C_2H_5)_2O$ was prepared by dehydration of [^{13}C]ethanol over $H_3PW_{12}O_{40}$ at 363 K. After purification by cryogenic vacuum distillation, diethyl ether containing 3% ethanol was obtained.

Reaction. Dehydration of ethanol was performed using a conventional flow reactor (8 mm i.d.) with 0.4–60 kPa of ethanol at 403 K in a He carrier under atmospheric pressure.[18-20] Prior to the reaction, $H_3PW_{12}O_{40}\cdot nH_2O$ was pretreated in a stream of He for 1 h at 423 K. After this treatment, n in $H_3PW_{12}O_{40}\cdot nH_2O$ was close to zero and the BET surface area was 6 $m^2\ g^{-1}$. The gases at the outlet of the reactor were analyzed by an on-line gas chromatograph (Shimadzu GC-8A, TCD, with a Porapak Q column).

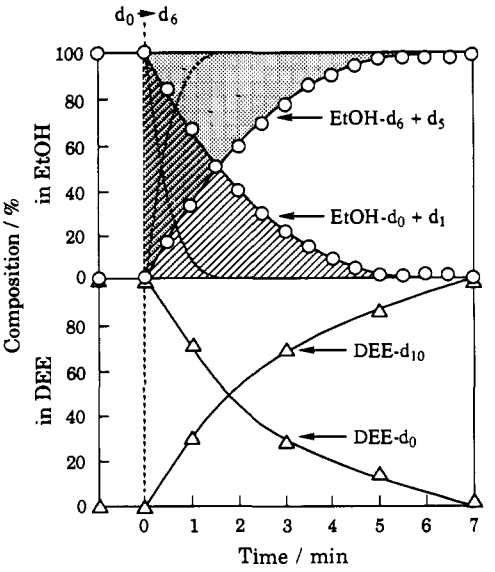

Figure 1. Transient-response at the outlet of the reactor to the replacement of the feed from ethanol-d_0 to -d_6 (16.4 kPa) during dehydration over $H_3PW_{12}O_{40}$ (403 K). At the vertical broken line, the feed was changed. See text for the broken and solid curves: top, ethanol (EtOH); bottom, diethyl ether (DEE).

Transient-Response Analysis. The uptake of ethanol into $H_3PW_{12}O_{40}$ under the working conditions was directly measured by means of a transient-response method as described previously.[18,19] After the reaction reached a stationary state, the feed gas was instantaneously changed from ethanol-d_0 to -d_6, and the variation of the isotopic composition of ethanol at the outlet was followed by a mass spectrometer (Anelva NAG-110). The changes of the product composition were also followed by the on-line gas chromatograph.

NMR Measurement. The samples for the NMR measurement were prepared using the closed circulation system. Prior to the absorption, liquid ethanol or diethyl ether was degassed by several freeze–pump–thaw cycles. The quantities of gases absorbed by $H_3PW_{12}O_{40}$ (ca. 0.5–1.0 g) were determined volumetrically. These quantities are expressed as the numbers of molecules absorbed per Keggin anion ($PW_{12}O_{40}^{3-}$). This expression is reasonable, since the chemical stoichiometry of absorption as well as IR spectra of absorption species assured that the solid bulk is nearly uniform. After the absorption, the sample was sealed and removed from the vacuum system. The sealed tube was opened in a dry bag under a N_2 atmosphere, transferred to a rotor, capped, and inserted into the NMR probe. The number of molecules remaining after the NMR measurement was determined by gas chromatography, after the samples were dissolved in water.

High-resolution solid-state NMR spectra were recorded at room temperature with magic angle spinning (MAS) on a Fourier transform pulsed NMR spectrometer (JEOL JNM-GX270) equipped with a CP/MAS unit (JEOL NM-GSH27MU).[34] ^{31}P MAS NMR spectra were taken at 109.2 MHz with and without cross polarization (CP) and with high power proton decoupling, while ^{13}C MAS NMR spectra were taken at 67.8 MHz with CP and proton decoupling. ^1H MAS NMR spectra were obtained at 270 MHz with a single pulse. ^{31}P chemical shifts were referenced to 15 mol dm^{-3} of H_3PO_4, and those for ^{13}C and ^1H to $(CH_3)_4Si$ (TMS).

Results

Pressure Dependency of Reaction Rate and Absorption Amount of Ethanol. The reaction rate and selectivity of the dehydration of ethanol over $H_3PW_{12}O_{40}$ changed slightly at the initial stage of the reaction, and reached stationary values after at least 1 h. The rate was proportional to the catalyst weight, and the product composition was constant below 60% conversion.

Figure 1 shows a typical result of the transient-response analysis carried out at 403 K and 16.4 kPa of ethanol. The changes in the isotopic compositions of ethanol and diethyl ether after the feed gas was instantaneously changed, at the stationary state from ethanol-d_0 to -d_6, are shown. The dotted lines indicate the results obtained in the absence of the catalyst (blank test) and the solid lines, the results in the presence of catalyst ($H_3PW_{12}O_{40}$). The content of ethanol-d_0 plus -d_1 (C_2H_5OH and C_2H_5OD) in the

(19) Misono, M.; Okuhara, T.; Ichiki, T.; Arai, T.; Kanda, Y. *J. Am. Chem. Soc.* **1987**, *109*, 5535–5536.

(20) (a) Hayakawa, N.; Okuhara, T.; Misono, M.; Yoneda, Y. *Nippon Kagaku Kaishi* **1982**, 356–363. (b) Okuhara, T.; Kasai, A.; Hayakawa, N.; Yoneda, Y.; Misono, M. *J. Catal.* **1983**, *83*, 121–130. (c) Okuhara, T.; Arai, T.; Ichiki, T.; Lee, K. Y.; Misono, M. *J. Mol. Catal.* **1989**, *55*, 293–301.

(21) Otake, M.; Onoda, T. *Shokubai (Catalyst)* **1976**, *18*, 169–179.

(22) (a) Okuhara, T.; Hibi, T.; Tatematsu, S.; Ichiki, T.; Misono, M. *9th Iberoamerican Symp. Catal.* **1984**, 623–632. (b) Saito, Y.; Niiyama, H. *J. Catal.* **1987**, *106*, 329–336.

(23) (a) Hibi, T.; Takahashi, K.; Okuhara, T.; Misono, M.; Yoneda, Y. *Appl. Catal.* **1986**, *24*, 69–83. (b) Okuhara, T.; Hibi, T.; Takahashi, K.; Tatematsu, S.; Misono, M. *J. Chem. Soc., Chem. Commun.* **1984**, 697–698.

(24) (a) Lee, K. Y.; Mizuno, N.; Okuhara, T.; Misono, M. *Bull. Chem. Soc. Jpn.* **1989**, *62*, 1731–1739. (b) Kanda, Y.; Lee, K. Y.; Nataka, S.; Asaoka, S.; Misono, M. *Chem. Lett.* **1988**, 139–142.

(25) Zardkoohi, M.; Haw, J. F.; Lunsford, J. H. *J. Am. Chem. Soc.* **1987**, *109*, 5278–5280.

(26) van den Berg, J. P.; Wolthuizen, J. P.; Clague, A. D. H.; Hays, G. R.; Huis, R.; van Hooff, J. H. C. *J. Catal.* **1983**, *80*, 130–138.

(27) Lombardo, E. A.; Dereppe, J. M.; Marcelin, G.; Hall, W. K. *J. Catal.* **1988**, *114*, 167–175.

(28) Bronnimann, C. E.; Maciel, G. E. *J. Am. Chem. Soc.* **1986**, *108*, 7154–7159.

(29) Kotanigawa, T.; Shimokawa, K.; Yoshida, T. *J. Chem. Soc., Chem. Commun.* **1982**, 1185–1187.

(30) Aronson, M. T.; Gorte, R. J.; Farneth, W. E.; White, D. *J. Am. Chem. Soc.* **1989**, *111*, 840–846.

(31) Knoth, W. H.; Farlee, R. D. *Inorg. Chem.* **1984**, *23*, 4765–4766.

(32) Farneth, W. E.; Starley, R. H.; Domaille, P. J.; Farlee, R. D. *J. Am. Chem. Soc.* **1987**, *109*, 4018–4023.

(33) Black, J. B.; Clayden, N. J.; Gai, P. L.; Scott, J. D.; Serwicka, E. M.; Goodenough, J. B. *J. Catal.* **1987**, *106*, 1–15.

(34) Lee, K. Y.; Mizuno, N.; Okuhara, T.; Misono, M.; Nakata, S.; Asaoka, S. *Chem. Lett.* **1988**, 1175–1178.

(35) Bronnimann, C. E.; Chuang, I.-S.; Hawkins, B. L.; Maciel, G. E. *J. Am. Chem. Soc.* **1987**, *109*, 1562–1564. Bronnimann, C. E.; Zeigler, R. C.; Maciel, G. E. *J. Am. Chem. Soc.* **1988**, *110*, 2023–2026.

(36) Maciel, G. E.; Haw, J. F.; Chuang, I.; Hawkins, B. L.; Early, T. A.; Mckay, D. R.; Pentakis, L. *J. Am. Chem. Soc.* **1983**, *105*, 5529–5535; Sindorf, D. W.; Macial, G. E. *J. Phys. Chem.* **1983**, *87*, 5516–5521.

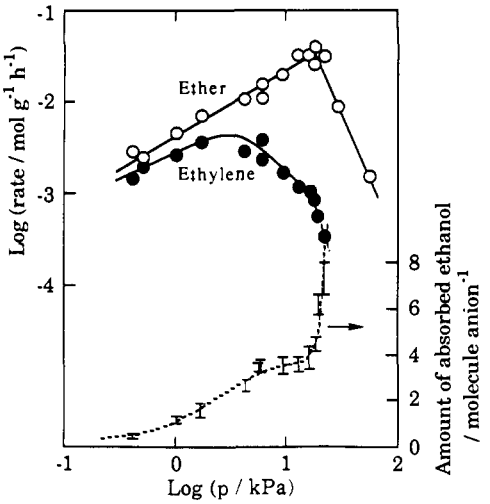

Figure 2. Rates of formation of diethyl ether and ethylene from ethanol over $H_3PW_{12}O_{40}$ (C_2-basis) as well as the amount of absorbed ethanol under the working conditions as a function of the partial pressure of ethanol:[19] reaction temperature, 403 K; W/F (ratio of the catalyst weight to the feed rate), 2–60 g h mol^{-1}.

outlet gas decreased and the content of C_2D_5OD plus C_2D_5OH increased in both cases, but the change was much slower in the presence of $H_3PW_{12}O_{40}$. Here, considering the rapid isotopic exchange for hydrogen atom of the OH group, C_2H_5OH and C_2H_5OD are considered to come from the d_0 species and C_2D_5OD and C_2D_5OH from the d_6 species. The change in the isotopic composition of diethyl ether was similar to that of ethanol, where the selectivity to diethyl ether was 96% under these reaction conditions. The isotopic composition of ethylene was not determined because of its low content.

The shaded area in Figure 1 corresponds to the amount of ethanol molecules ($d_0 + d_1$) which had been held by the $H_3PW_{12}O_{40}$ before the change of the fed alcohol. The dotted area, on the other hand, corresponds to the amount of ethanol ($d_6 + d_5$) that was newly held by the catalyst. These two values naturally agreed and correspond to the amount of ethanol held by $H_3PW_{12}O_{40}$ under the stationary working conditions. In the case of Figure 1, the amount of ethanol held by $H_3PW_{12}O_{40}$ was 4.3 molecules per Keggin anion (in the bulk and on the surface), as calculated from the shaded or dotted area. This large value clearly shows that the ethanol molecules are mostly absorbed in the bulk as will be discussed later.

The pressure dependencies of the rates of formation of diethyl ether and ethylene as well as the amounts of ethanol absorbed obtained by the above method are shown in Figure 2.[19] Initially, the rate of the ethylene formation increased with the ethanol pressure by about one-half order to the partial pressure, and then decreased significantly at higher pressures. The rate of the diethyl ether formation changed similarly, but the maximum rate was observed at a much higher pressure than ethylene formation. The reaction order of the diethyl ether formation was about 0.8 at the lower pressure region.

The quantity of absorbed ethanol is shown by the units of the number of ethanol molecules per Keggin anion in the whole bulk on the right-hand ordinate of Figure 2. The amounts increased from 0.4 to 8.0 molecules per anion as the partial pressure of ethanol increased from 0.4 to 60 kPa. The amounts correspond to 4–80 times the amount needed to form monolayer adsorption. It is noteworthy that the amounts were about 3 and 6 molecules per anion (1 and 2 molecules per proton) at the pressures giving maximum formation of ethylene and ether, respectively.

Absorption/Desorption of Ethanol in $H_3PW_{12}O_{40}$. Alcohol and ether were readily absorbed by $H_3PW_{12}O_{40}$, and the quantity absorbed tended to be discrete values, that is, multiples of protons.[15,16] As shown in Figure 3, a state of $H_3PW_{12}O_{40}\cdot 3C_2H_5OH$ (ethanol/anion = 3; ethanol/H^+ = 1) was brought about at 0.27 kPa of ethanol at 318 K. By increasing the pressure to 0.67 and

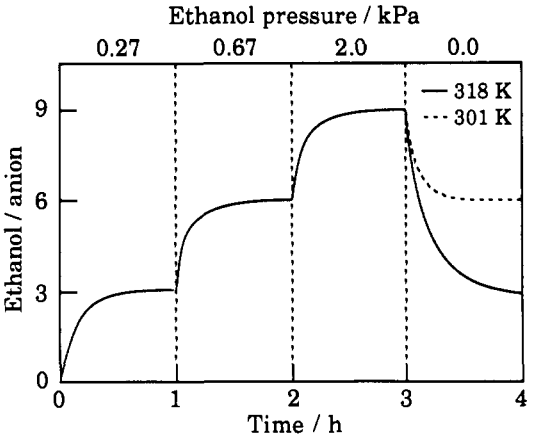

Figure 3. Change of absorption amount in $H_3PW_{12}O_{40}$ by the pressure jump of ethanol.

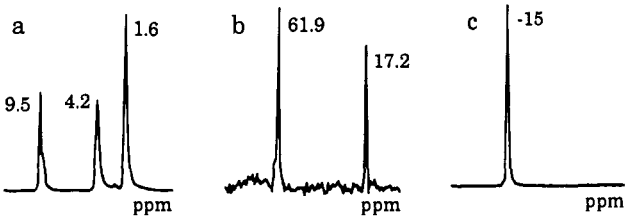

Figure 4. Solid-state NMR spectra of $H_3PW_{12}O_{40}\cdot 6C_2H_5OH$: (a) ^1H, (b) ^{13}C, and (c) ^{31}P NMR.

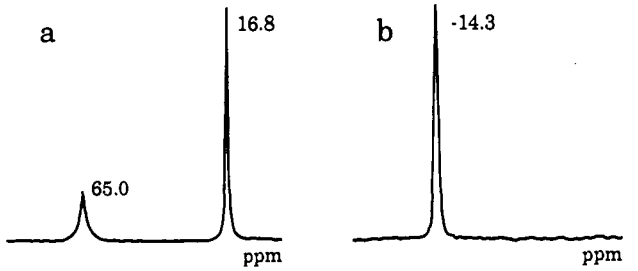

Figure 5. Solid-state NMR spectra of $H_3PW_{12}O_{40}\cdot 3C_2H_5OH$: (a) ^{13}C, (b) ^{31}P NMR.

2.0 kPa at the same temperature, $H_3PW_{12}O_{40}\cdot 3C_2H_5OH$ changed to $H_3PW_{12}O_{40}\cdot 6C_2H_5OH$ (ethanol/anion = 6; ethanol/H^+ = 2) and $H_3PW_{12}O_{40}\cdot 9C_2H_5OH$. Subsequent evacuation at 301 and 318 K produced $H_3PW_{12}O_{40}\cdot 6C_2H_5OH$ and $H_3PW_{12}O_{40}\cdot 3C_2H_5OH$, respectively.

Solid-State NMR and IR of $H_3PW_{12}O_{40}\cdot n C_2H_5OH$. Solid-state NMR spectra for $H_3PW_{12}O_{40}\cdot 6C_2H_5OH$ that were reported previously[24b] are shown in Figure 4. It should be noted that three sharp peaks in the ^1H NMR spectrum appeared at 9.5, 4.2, and 1.6 ppm. The half-widths of the peaks were less than 80 Hz. It was observed that these ^1H peaks were sensitive to the amount of ethanol molecules absorbed; no distinct ^1H peaks were detected for $H_3PW_{12}O_{40}$ having less than 6 molecules of ethanol per anion. In the ^{13}C NMR (Figure 4b), two sharp peaks were observed at 61.9 and 17.2 ppm, which corresponded to CH_2 and CH_3 groups, respectively (vide infra). The ^{31}P NMR spectrum gave a sharp and symmetric peak at −15.0 ppm (half-width, 60 Hz) (Figure 4c).

The ^{13}C and ^{31}P solid-state NMR spectra of $H_3PW_{12}O_{40}\cdot 3C_2H_5OH$ are given in Figure 5. The ^1H NMR spectrum of this sample was not detected, as described above. Figure 5a shows that the CH_3 peak was shifted upfield by 0.4 ppm and the CH_2 downfield by 3.1 ppm from those of $H_3PW_{12}O_{40}\cdot 6C_2H_5OH$. The ^{31}P NMR peak appeared at −14.3 ppm, downfield by 0.7 ppm (Figure 5b).

Figure 6 shows the IR data of $H_3PW_{12}O_{40}$ containing 3 or 6 molecules of ethanol and diethyl ether.[24a] Two bands at 1442 cm^{-1} (CH_3 degenerate deformation) and 1388 cm^{-1} (CH_3 symmetric

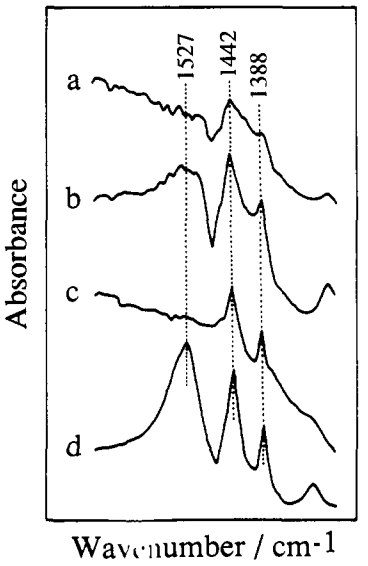

Figure 6. IR spectra for (a) $H_3PW_{12}O_{40}\cdot 3C_2H_5OH$, (b) $H_3PW_{12}O_{40}\cdot 6C_2H_5OH$, (c) $H_3PW_{12}O_{40}\cdot 3(C_2H_5)_2O$, and (d) $H_3PW_{12}O_{40}\cdot 6(C_2H_5)_2O$.

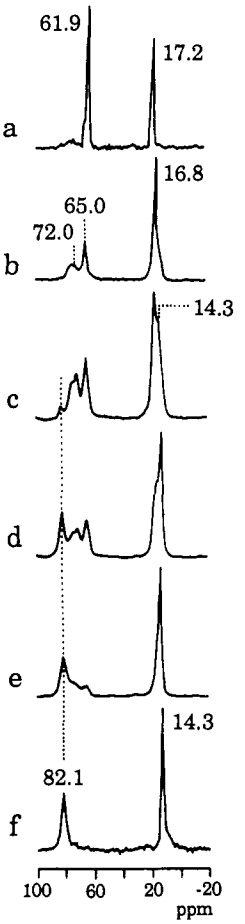

Figure 7. Transformation of protonated ethanol dimer in $H_3PW_{12}O_{40}$ by heat treatment. Solid-state ^{13}C CP/MAS NMR spectra were obtained using high-purity ^{13}C ethanol: (a) dimer, (b) 333 K, (c) 343 K, (d) 363 K, (e) 373 K, (f) 423 K.

deformation and CH_2 wagging vibration) were observed. In addition, a broad band at 1527 cm^{-1} was observed for $H_3PW_{12}O_{40}\cdot 6C_2H_5OH$ and $H_3PW_{12}O_{40}\cdot 6(C_2H_5)_2O$. This band was not observed from $H_3PW_{12}O_{40}\cdot 3C_2H_5OH$ and $H_3PW_{12}O_{40}\cdot 3(C_2H_5)_2O$.

Changes in the NMR Spectra of Ethanol in $H_3PW_{12}O_{40}$ upon Heat Treatment. The transformation of ethanol absorbed by $H_3PW_{12}O_{40}$ upon heat treatment was followed by solid-state ^{13}C NMR; the results are shown in Figure 7. The most intense peak

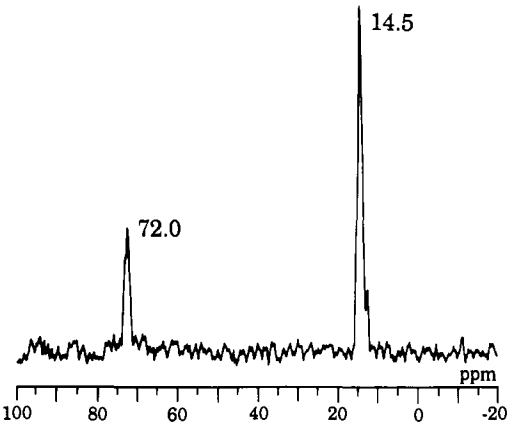

Figure 8. ^{13}C NMR spectra of $H_3PW_{12}O_{40}\cdot 3(C_2H_5)_2O$.

Table I. Thermal Desorption of Absorbed Ethanol in $H_3PW_{12}O_{40}$

			gas-phase produts/ C_2 per anion		
temp/K	treatment	absorbed amount[a]/ C_2 per anion	ethanol	diethyl ether	ethylene
		Run 1			
(1) 298	^{12}C-abs	8.70			
(2) 298	evac	5.81	2.89	0	0
(3) 323	evac	4.78	1.03	0	0
(4) 348	evac	2.05	2.63	0	0.10
(5) 298	^{13}C-abs	12.01			
(6) 298	evac	5.90	7.74	0.42[b]	0
		Run 2			
(1) 298	abs	8.90			
(2) 298	evac	5.94	2.96	0	0
(3) 323	evac	4.83	1.11	0	0.09
(4) 348	evac	2.09	2.65	0	0.98
(5) 373	evac	0.90	0.21	0	0.40
(6) 423	evac	0.50	0	0	0

[a] The amount of C_2 species that was held by $H_3PW_{12}O_{40}$ after the treatment. [b] $(^{12}C_2H_5)_2O$, 90%.

in each spectrum is drawn in this figure to have the same height. For this measurement, $^{13}C_2H_5OH$ (^{13}C, 99%) was used in order to take the spectra in a much shorter time to avoid the undesirable increase of sample temperature.

When $H_3PW_{12}O_{40}\cdot 6C_2H_5OH$ (Figure 7a) was evacuated at 333 K for 1 h, two peaks appeared at 65.0 and 16.8 ppm, which were the same as those of $H_3PW_{12}O_{40}\cdot 3C_2H_5OH$ (Figure 5a), together with new peaks at 72.0 and about 14.5 ppm (Figure 7b). By further evacuation at 343 K, the relative intensities of the latter set of peaks increased, and an additional new set of peaks was observed at 82.1 and about 14.3 ppm (Figure 7c). The peak around 15 ppm was much broader than that of $H_3PW_{12}O_{40}\cdot 6C_2H_5OH$ due to the overlapping of the peaks at 14–17 ppm. The peaks at 82.1 and 14.3 ppm became predominant at 363 K (Figure 7d) and were the only ones that grew in intensity after evacuation at 423 K (Figure 7f).

In Figure 8, the ^{13}C NMR spectrum of $H_3PW_{12}O_{40}\cdot 3(^{13}C_2H_5)_2O$ is given, which was prepared by the absorption of $(^{13}C_2H_5)_2O$ into $H_3PW_{12}O_{40}$ at 298 K and the subsequent evacuation at 323 K. Two peaks were detected at 72.0 and 14.5 ppm.

Thermal Desorption of Absorbed Ethanol. To reveal the reactions during the heat treatment, thermal desorption of absorbed ethanol was performed, and the results are summarized in Table I. Initially, about 9 molecules of ethanol ($^{12}C_2H_5OH$) per anion of $H_3PW_{12}O_{40}$ was absorbed at 298 K upon exposure to ethanol vapor (line 1 of run 1). After vapor-phase molecules were trapped by liquid N_2 for 1 h (here, this procedure is called evacuation), about 6 molecules of ethanol per anion was found to remain in the bulk phase. The product that desorbed into the gas phase (collected by the liquid N_2 trap) contained only ethanol (2.89 molecules/anion). Gas that desorbed between 298–323 and 323–348 K was identified as ethanol (1.03 and 2.63), and no

diethyl ether was detected. After heating to 348 K, the number of molecules remaining in $H_3PW_{12}O_{40}$ became 2.05 per anion (C_2-basis, line 4).

To $H_3PW_{12}O_{40}$ containing 2.05 molecules per anion, about 10 molecules of $^{13}C_2H_5OH$ per anion was added to the bulk at 298 K. The ^{13}C to ^{12}C ratio for molecules in the bulk then became 4.9:1. The gases that desorbed at 298 K were trapped for 1 h and analyzed by GC and GC–MS spectroscopy. The trapped gases were identified as 7.74 ethanol and 0.42 diethyl ether molecules per anion (C_2-basis), and the remainder in $H_3PW_{12}O_{40}$ was 5.90 molecules per anion (line 6) (close to 5.81 (line 2)). Diethyl ether, which was not desorbed during the initial thermal desorption (lines 1 to 4), was obtained in this step. The isotopic composition of the diethyl ether collected was 90% $(^{12}C_2H_5)_2O$, 6% $^{13}C_2H_5O^{12}C_2H_5$, and 4% $(^{13}C_2H_5)_2O$. This isotopic composition (mostly ^{12}C) implies that the diethyl ether was produced mainly from the ethanol that was introduced by the first absorption (line 1). The temperature was then raised to 348 K, collecting the gas phase with the liquid N_2 trap. The ratio of ^{13}C:^{12}C for the products collected at 298 K plus those between 298 and 348 K was 4.7:1. This value is comparable to the isotopic ratio of ethanol in the bulk before desorption (4.9:1).

Another similar experiment was carried out for the sample that preabsorbed ethanol and experienced thermal desorption. In this experiment, the maximum temperature for the initial thermal desorption was 323 K (the same treatment as in lines 1 to 3 of run 1, Table I) instead of 348 K. When ethanol was introduced after the initial thermal desorption to this sample at 298 K and subsequently evacuated, no diethyl ether was detected in the trapped gases, in contrast with the sample which experienced 348 K.

In Table I (run 2), the product distribution of ordinary thermal desorption of ethanol is also given. The temperature was raised stepwise to 423 K. Up to 348 K, results similar to run 1 were obtained. Ethylene appeared at 348 K and showed a maximum at 373 K. Diethyl ether was not detected in the gas phase during the whole thermal desorption process as reported previously.[20b]

Discussion

Unusual Pressure Dependency of Dehydration of Ethanol. Kinetic studies of ethanol dehydration have been reported for typical solid acids such as Al_2O_3 and SiO_2–Al_2O_3.[37-39] Roca et al. reported zero order for ethylene formation and between zero and first order for ether formation over SiO_2–Al_2O_3 at 453 K.[39a] For SiO_2–Al_2O_3, Take et al.[39b] observed that the reaction orders were 0–1 and 0.4–0.7 for the formations of ethylene and ether, respectively. Furthermore, over Al_2O_3, the reaction order of formation of ethylene was zero and that of ether, 1 (2.7–12.0 kPa) to 2 (0–2.7 kPa).[38]

The pressure dependency observed in the present study for $H_3PW_{12}O_{40}$ (Figure 2) was very different from those for the ordinary solid acids described above. This peculiar pressure dependency is reasonably explained by the pseudoliquid phase model, as previously suggested.[19] We have shown for the dehydration of 2-propanol over $H_3PW_{12}O_{40}$ at 353 K that a large amount of 2-propanol was held in $H_3PW_{12}O_{40}$ under the working conditions and the rate of absorption–desorption was much faster than the rate of dehydration.[18] Therefore, it appeared that the reaction took place in the bulk phase. Since the amount of ethanol held by $H_3PW_{12}O_{40}$ under the reaction conditions in the present work (Figure 2) was 4–80 times the amount for a monolayer, it is obvious that $H_3PW_{12}O_{40}$ is also in the state of the pseudoliquid phase during the dehydration of ethanol.

Noteworthy observations in Figure 2 are that (i) the reaction rate apparently varies corresponding to the changes in the amount of absorbed ethanol, (ii) ethylene is preferably formed at low ethanol to proton ratio, and (iii) ether formation is favored as this ratio increases. Thus, eqs 1–3 can be considered as plausible reaction steps.

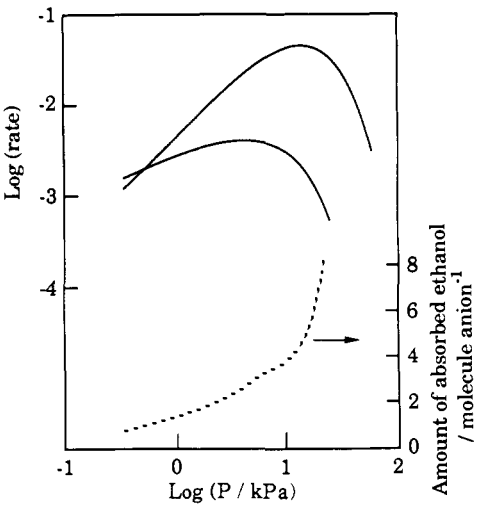

Figure 9. Calculated pressure dependency of ethanol dehydration over $H_3PW_{12}O_{40}$ (compare with the results in Figure 2).

$$C_2H_5OH + H^+ \underset{}{\overset{K_1}{\rightleftharpoons}} \underset{(I)}{C_2H_5OH_2^+} \xrightarrow{k_1} C_2H_4 + H_2O + H^+ \quad (1)$$

$$C_2H_5OH + \underset{(I)}{C_2H_5OH_2^+} \overset{K_2}{\rightleftharpoons} \underset{(II)}{(C_2H_5OH)_2H^+} \xrightarrow{k_2} (C_2H_5)_2O + H_2O + H^+ \quad (2)$$

$$(n-2)C_2H_5OH + \underset{(II)}{(C_2H_5OH)_2H^+} \overset{K_3}{\rightleftharpoons} \underset{(III)}{(C_2H_5OH)_nH^+} \cdots\cdots (n\geq 3, \text{inactive}) \quad (3)$$

In this model, it is assumed that ethylene is formed from a protonated monomer, I, ether from a protonated dimer, II, and $(C_2H_5OH)_nH^+$ ($n \geq 3$), III, being much less reactive. As will be discussed in the next section, the presence of I and II in the pseudoliquid phase was shown by the present NMR study. The concentration of protonated ethanol is determined by the protonation equilibria. As the partial pressure of ethanol increases, the major species in the pseudoliquid phase would vary from I to the oligomer, III, through II. When the pressure exceeded about 15 kPa, the amount of absorbed ethanol increased rapidly and the rate decreased markedly. Hence, the phase with a high concentration of ethanol is not active, in accordance with the assumption that the oligomer is not reactive.

We also attempted to simulate the pressure dependency observed experimentally (Figure 2). The rates of ethylene and ether formation as well as the absorbed ethanol were calculated based on eqs 1–3. It was assumed that I, II, and III are in equilibrium. The total amount of absorbed ethanol is (monomer + 2 × dimer + n × oligomer). Considering the equilibrium constants (K_1, K_2, and K_3), rate constants (k_1 and k_2), and n as variables, the simulation was optimized by the least squares method. Figure 9 shows the optimized result, where n = 5, k_1 (g^{-1} h^{-1}) = 0.002, k_2 (g^{-1} h^{-1}) = 0.032, K_1 (kPa^{-1}) = 6.8 × 10^{-4}, K_2 (kPa^{-1}) = 8.8 × 10^{-5}, and K_3 (kPa^{-3}) = 9.5 × 10^{-12}. The trends of the changes in the rates and the absorption amounts in Figure 2 were essentially reproduced, thus, supporting the proposed mechanism shown by eqs 1–3.

The results previously observed for the dehydration of 2-propanol are in agreement with the above concept. There were two different "pseudoliquid phases" having different amounts of absorption (about 3 and 6–8 molecules of 2-propanol per anion) and correspondingly two different catalytic activities and selectivities.[40] The transition between the two "psuedoliquid phases" took place reversibly at 373 K.

(37) Pines, H.; Manassen, J. *Adv. Catal.* **1966**, *16*, 49–93.
(38) Knozinger, H. *Angew. Chem., Int. Ed. Engl.* **1968**, *7*, 791–805.
(39) (a) Figueras Roca, F.; De Mourgues, L.; Trambouze, Y. *J. Catal.* **1969**, *14*, 107–113. (b) Take, J.; Yoneda, Y. *Shokubai (Catalyst)* **1965**, *7*, 317–320. (c) de Boer, J. H.; Fahim, R. B.; Linsen, B. G.; Visseren, W. J.; de Vleesshawer, W. F. N. M. *J. Catal.* **1967**, *7*, 163–172.

(40) Takahashi, K.; Okuhara, T.; Misono, M. *Chem. Lett.* **1985**, 841–842.

Table II. Chemical Shifts of ^1H NMR for OH of Ethanol Protonated in Superacids

superacids[a]	temp/K	chemical shift/ ppm from TMS	ref
$HF + BF_3$	203	8.25	42a
$FSO_3H/SbF_5/SO_2$	213	9.30	42b
HSO_3F	178	9.89	42c
$HBr + CBr_2F_2$	153	12.06	42d

[a] H_0: HF (−10.2), HSO_3F (−15.07), FSO_3H/SbF_5 (−20).

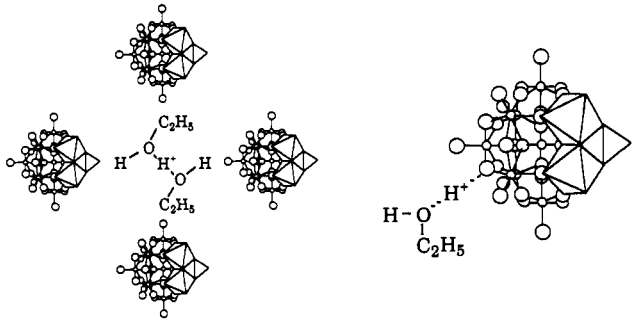

Figure 10. Structures of protonated ethanol dimer and monomer.

Protonated Ethanol in the Pseudoliquid Phase. The chemical states of absorbed ethanol in the pseudoliquid phase, which are assumed in eqs 1–3 as reaction intermediates, will be discussed on the basis of the results of solid-state NMR studies. As shown in Figure 4a, $H_3PW_{12}O_{40}\cdot 6C_2H_5OH$ gave well-resolved ^1H NMR spectra. This is, to our knowledge, the first example in which a well-resolved solid-state ^1H NMR spectrum was observed for protonated organic compounds in the solid state. The pseudoliquid phase is responsible for the well-resolved ^1H NMR spectra. The high resolution is probably due to (a) the high mobility of the activated ethanol and (b) homogeneity of the bulk phase.

It is well known that the chemical shift of the hydroxyl proton is greatly influenced by hydrogen bonding. In the case of a dilute ethanol solution, the ^1H chemical shift for the hydroxyl proton is 1.0 ppm.[41] On the other hand, protonated ethanols in superacid solutions such as FSO_3H/SbF_5 show chemical shifts in the range of 9–12 ppm as are summarized in Table II. The chemical shift of the OH proton in $H_3PW_{12}O_{40}\cdot 6C_2H_5OH$ (9.5 ppm) is in agreement with those in the superacid. Therefore, ethanol molecules in $H_3PW_{12}O_{40}\cdot 6C_2H_5OH$ are protonated ethanols, $(C_2H_5OH)_2H^+$, and in this respect, $H_3PW_{12}O_{40}$ may be regarded as a "solid superacid". The ^1H NMR peaks at 4.2 and 1.6 ppm (CH_2 and CH_3, respectively) are slightly shifted from those of liquid ethanol (CH_2, 3.6 ppm; CH_3, 1.2 ppm).[41] The relative intensity ($OH/CH_2/CH_3$ = 1.45:1.8:3.0) as well as the stoichiometry of ethanol to proton (2:1) indicates that this species is the protonated ethanol dimer, $(C_2H_5OH)_2H^+$ (II). We have previously reported that the 1527-cm^{-1} band in $H_3PW_{12}O_{40}\cdot 6C_2H_5OH$ is due to the OH stretching band in $C_2H_5(H)O\cdots H^+\cdots O(H)C_2H_5$.[24a] The probable structure of $H_3PW_{12}O_{40}\cdot 6C_2H_5OH$ is shown in Figure 10.

The peaks of ^{13}C NMR for the dimer, 61.9 and 17.2 ppm, can be assigned to CH_2 and CH_3, respectively (cf. 57.0 and 17.6 ppm for CH_2 and CH_3 in neat C_2H_5OH[43]).

In the case of $H_3PW_{12}O_{40}\cdot 3C_2H_5OH$, no clear ^1H NMR signal was observed. This is probably due to the low mobility induced by the stronger interaction with polyanion. From IR data, the structure of the monomer species has previously been proposed to be an ethanol molecule hydrogen-bonded to the bridging oxygen of the anion.[24a] The chemical shifts of both ^{31}P and ^{13}C are distinctly different from those of the protonated dimer, II. Considering the IR data (Figure 6)[24a] and the stoichiometry of ethanol to proton (1:1), the signals are assigned to protonated ethanol monomer ($C_2H_5OH_2^+$, I). The formations of protonated monomer and dimer have been shown in the case of pyridine absorbed by $H_3PW_{12}O_{40}$.[15] Thus, the unique absorption states with 3 and 6 ethanol molecules per anion observed in the absorption experiment (Figure 3)[16] correspond to the formations of protonated ethanol monomer and dimer by the stoichiometric reactions of absorbed ethanol with $H_3PW_{12}O_{40}$ in the bulk state.

Transformation of the Protonated Species. As discussed in the previous sections, protonated ethanol species may be involved in the catalytic dehydration of ethanol. The quantities of ethanol absorbed and the molecules produced in the bulk during the heat treatment are calculated based on the ^{13}C NMR peak intensities of Figure 7, as shown in Table III. By evacuation at 333 K, the protonated dimer species (II) changed to monomer (I) (65.0 and 16.8 ppm) and another species (72.0 and ca. 14.5 ppm), accompanied by the desorption of ethanol. If one considers that $H_3PW_{12}O_{40}\cdot 3(C_2H_5)_2O$ gave peaks at 72.0 and 14.5 ppm (Figure 8) in the ^{13}C NMR spectrum, the new species is assigned to protonated ether. The presence of protonated ether in $H_3PW_{12}O_{40}\cdot 3(C_2H_5)_2O$ has previously been inferred by IR data.[24a]

When the sample was heated to 343–423 K, peaks at 82.1 and 14.3 ppm were observed (Figure 7, c to f) in the ^{13}C NMR spectrum. The ^{13}C chemical shift of CH_2 at 82.1 ppm is significantly downfield from that of ethanol (57.0 ppm). Farneth et al.[32] has reported that when methanol adsorbed on $K_{3-x}H_xPMo_{12}O_{40}$ was heated at 423 K, the CH_2 peak shifted from 51 to 75 ppm, and this change was assigned to the transformation of adsorbed methanol to methoxide. The extent of this shift is comparable to that of CH_2 in the present study. Therefore, the species we observed (Figure 7f) may be assigned to ethoxide. In accordance with this assignment, the ^{31}P NMR spectrum showed a peak at −12.3 ppm,[34] in good agreement with that of $(C_2H_5O)_3PW_{12}O_{37}$ which has been reported by Knoth et al.[31] The formation of ethoxide has also been suggested by IR data under the same conditions.[24a]

Between 333 and 343 K, not only ethoxide in the bulk phase but also ethylene in the gas phase was produced, accompanied by a decrease in protonated ethanol formation (Table III). The amount of the protonated ether, however, changed little. It was observed that the ether absorbed did not give ethanol or ethylene in the gas phase below 343 K.[24a] These facts indicate that ethylene or ethoxide was formed from protonated ethanol monomer above 333 K, while protonated ether, once produced in the bulk, hardly reacted or was desorbed below 343 K.

Above 343 K, ethylene was further desorbed and the formation of ethoxide increased, while the NMR data showed that the ratios of ethanol monomer to protonated ether were almost unchanged in this region (343 K, 0.85; 363 K, 0.82; 373 K, 0.79). Hence, ethylene and ethoxide were produced from both the ethanol monomer and protonated ether above 343 K.

Bradley et al. have reported the ^{13}C NMR chemical shifts for CH_3 and CH_2 of tungsten ethoxide ($W(OCH_2CH_3)_6$) to be 18.8 and 69.8 ppm, respectively.[44] The CH_2 group of ethoxide in the present study (82.1 ppm) appeared about 12 ppm downfield from tungsten ethoxide, indicating that the species observed in this study is more positively charged. However, according to Olah et al., *sec*-propyl and *tert*-butyl cations in a superacid solution gave peaks at 320.6 and 335.2 ppm for this α-carbon, respectively.[45] These

(41) Bovey, F. A. *Nuclear Magnetic Resonance Spectroscopy*; Academic Press: New York, 1969; pp 82–85.

(42) (a) Maclean, C.; Mackor, E. L. *J. Chem. Phys.* **1961**, *34*, 2207–2208; *Discuss. Faraday Soc.* **1962**, *34*, 165–176. (b) Olah, G. A.; Namanworth, E. *J. Am. Chem. Soc.* **1966**, *88*, 5327–5328. Olah, G. A.; Sommer, J.; Namanworth, E. *J. Am. Chem. Soc.* **1967**, *89*, 3576–3581. (c) Birchall, T.; Gillespie, R. J. *Can. J. Chem.* **1965**, *43*, 1045–1051. (d) Emsley, J.; Gold, V.; Jais, M. J. B. *J. Chem. Soc., Chem. Commun.* **1979**, 961–962. Emsley, J.; Gold, V.; Hibbert, F.; Jais, M. J. B. *J. Chem. Soc., Perkin Trans. 2* **1986**, 1279–1281.

(43) Breitmaier, E.; Voelter, W. *Carbon-13 NMR Spectroscopy*; VCH Publishers: Weinheim, 1987; p 208.

(44) Bradley, D. C.; Chisholm, M. H.; Extine, M. W.; Stager, M. E. *Inorg. Chem.* **1977**, *16*, 1794–1801.

(45) Olah, G. A.; Prakash, G. K. S.; Sommer, S. *Superacids*; John Wiley: New York, 1985; p 80.

Table III. Amounts of Absorbed Molecules as Well as Produced Molecules in the Bulk and Gas Phase during the Heat Treatment Based on the ^{13}C NMR Results of Figure 7

treatment temp/K	absorbed amount/ C_2 per anion	products/C_2 per anion: gas phase ethanol	gas phase ethylene	bulk $(C_2H_5OH)_2H^+$ (65.0 ppm)	bulk $C_2H_5OH_2^+$ (61.9 ppm)	bulk $(C_2H_5)_2OH^+$ (72.0 ppm)	bulk C_2H_5O– (82.1 ppm)
a (298)	5.98			5.98	0	0	0
b (333)	2.75	3.23	0	0	1.57	1.18	0
c (343)	2.25	0.47	0.03	0	0.99	1.17	0.09
d (363)	2.05	0.12	0.08	0	0.59	0.72	0.74
e (373)	0.95	0.20	0.90	0	0.15	0.19	0.61
f (423)	0.50	0	0.45	0	0	0	0.50

Scheme I. Reaction Scheme for Ethanol Dehydration in Pseudoliquid Phase

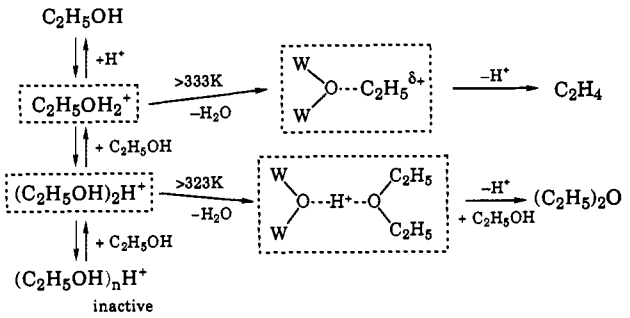

are shifted about 260 ppm downfield from the corresponding alcohols ($(CH_3)_2{}^{13}CHOH$, 63.4 ppm; $(CH_3)_3{}^{13}COH$, 68.4 ppm).[43] Therefore, the species observed here is more like ethoxide than free ethyl cation, although the ethyl group is more positively charged than ordinary ethoxide.

Formation of Diethyl Ether in Bulk. In the thermal desorption of ethanol absorbed in the bulk of $H_3PW_{12}O_{40}$, ether was not desorbed in the gas phase, and only ethylene was observed, as shown in Table I (run 2, (1)–(4))[20b] (in contrast to the thermal desorption from ethanol adsorbed on Al_2O_3[46]). On the other hand, ether was formed mainly in the *catalytic* dehydration of ethanol over $H_3PW_{12}O_{40}$. Thus we had speculated that ethylene was formed from ethanol absorbed in the bulk and ether was formed on the surface.[20b] However, the ^{13}C NMR in the present study showed the formation of diethyl ether in the bulk (Figure 7, b–d) and that diethyl ether was desorbed in the gas phase when ethanol was introduced (Table I, line 6 of run 1). The isotopic composition of ether desorbed showed that it had already been produced in the bulk during the preceding thermal desorption (this diethyl ether was formed between 323 and 348 K, since it was not detected in the 323-K-treated sample, but for the 348-K-treated sample). It is likely that these ether molecules are strongly held by the heteropoly acid and cannot desorb by the simple thermal desorption below 348 K, but can desorb by the replacement with ethanol molecules. This is consistent with the formation of ether during the catalytic dehydration of ethanol over $H_3PW_{12}O_{40}$.

Reaction Mechanism of Ethanol Dehydration in the Pseudoliquid Phase. Based on the above discussion, a revised and more detailed mechanism as in Scheme I may be proposed for the main reaction paths of the thermal desorption of ethanol. The species which were observed directly in the present study are surrounded by broken lines. Below 323 K, the dehydration does not proceed, and only reversible absorption and desorption take place. The protonated ethanol dimer is transformed into protonated ether above 323 K and then to diethyl ether by the replacement with ethanol. Protonated ethanol monomer gives ethylene via ethoxide above 333 K.

If one considers the computer simulation based on the proposed reaction scheme (eqs 1–3) (Figure 9) and the transient-response analysis (Figures 1 and 2), ethanol dehydration likely takes place in the same manner as in the Scheme I.

Conclusion

(1) A large quantity of ethanol was absorbed in the lattice of the catalyst bulk (pseudoliquid phase) under the reaction conditions and the reaction proceeded in this phase.

(2) Probable reaction intermediates of the ethanol dehydration such as protonated ethanol dimer ($(C_2H_5OH)_2H^+$), monomer ($C_2H_5OH_2^+$), protonated ether, and ethoxide were directly identified in this phase by solid-state NMR and IR spectroscopy and stoichiometry of ethanol absorption.

(3) The dimer and monomer species are mainly transformed to diethyl ether and ethylene through protonated ether and ethoxide, respectively.

(4) An unusual pressure dependence observed for the dehydration of ethanol was reasonably explained by the changes in the amounts of these intermediates in the pseudoliquid phase. This behavior must be closely related to catalytic selectivity as well as high activity reported in the literature.[5]

(46) Arai, H.; Take, J.; Saito, Y.; Yoneda, Y. *J. Catal.* **1967**, *9*, 146–153.